Model of Bacteria Mutualism in a Chemostat: Analysis and Optimization with Interval Detector

Juan Carlos Arceo, Olivier Bernard, Jean-Luc Gouzé

Model of Bacteria Mutualism in a Chemostat: Analysis and Optimization with Interval Detector

Juan Carlos Arceo, Olivier Bernard, and Jean-Luc Gouzé

***Abstract*—This work focuses on a model of two bacteria growing and exchanging nutrients in a chemostat. Bacterial uptake rate is described via Michaelis-Menten equations; we assume a constant yield and metabolite production directly proportional to bacterial growth. We analyse the model via a reduced order system, then, conditions to determine existence and global stability of the equilibria are given in terms of the dilution rate. Finally, bacterial productivity is maximized; an interval detector is designed to estimate this productivity and an optimization strategy for periodic dilution rates is proposed.**

***Index Terms*—Bacteria, Interval detector, Metabolite cross-feeding, Mutualism, Optimization**

I. Introduction

Symbiosis is a concept employed to describe organisms living in a close association [1]; mutualism is a type of symbiosis that has been described as the interaction of species in which they obtain benefits from each other [2], [3]. In [4] an instance of mutualism (syntrophy) was modeled and analysed, in the syntrophic case at least one of the organisms can grow without the other. Examples of mutualism are found in plants and seed dispersers [5], or metabolic cross-feeding [6], defined as the interaction in which a bacteria consumes the metabolite produced by another bacteria. In this article we present the model, analysis and optimization of two bacteria under metabolic cross-feeding in a continuous chemostat.

We focus on a generic structure that characterizes a loop in an ecosystem. The structure is very general and can represent at least partially systems including such a loop: primary producers of detritic matter recycled by bacteria into nutrients [7]; oxygen produced by phytoplankton is consumed by bacteria, and it produces CO_2 to feed the phytoplankton [8].

Our contributions consist in 1) proposing a new model for mutualism 2) studying its global stability, 3) an application of monotone systems theory to derive interval detectors 4) the optimization of bacterial productivity via signal averaging.

The manuscript is organized as follows: section II presents a model for mutualistic interaction among two bacteria in a chemostat; in section III the model solutions are analysed, a model reduction is performed by means of the mass conservation principle, then, its steady-state, local and global stability are studied in terms of the chemostat dilution rate; in section IV the optimal dilution rate and substrate production term that maximizes bacterial productivity at steady-state are computed; in section V an interval detector is designed to estimate upper and lower bounds of the unmeasured states; in section VI an approach for steady-state optimization using the interval detector is presented; finally, in section VII a conclusion is given, as well as perspectives for future works are established.

Acknowledgements. This research work has received support from the ANR Projects Ctrl-AB (ANR-20-CE45-0014), PhotoBiofilm Explorer (ANR-20-CE43-0008) and ANR Project Maximic (ANR-17-CE40-0024).

J.C.A., O.B. and J.-L.G., are with Université Côte d'Azur, Inria, INRAE, CNRS, Sorbonne Université, Biocore team, Sophia Antipolis, France, (Emails: juan-carlos.arceo-luzanilla@inria.fr, olivier.bernard@inria.fr, jean-luc.gouze@inria.fr)

II. System description and modeling

In this section we describe the system to be modeled. First, consider the chemostat [9] whose scheme is shown in Fig. 1; the tank volume is $V\left(m^3\right)$, the inflow and outflow are denoted $F\left(t\right)$ (volume/time), the dilution rate is obtained by dividing the flow by the tank volume $d\left(t\right)$=$F\left(t\right)/V\left(1/\text{time}\right)$; the inflow contains two nutrients whose concentration are s_1^{in} and s_2^{in}; moreover, there are two bacteria population inside the bioreactor x_1 and x_2 (mass/volume). Time dependency of the variables is dropped thereafter for notation simplicity. We assume that the bacteria x_1 is growth-limited by the substrate s_1, and it produces substrate s_2 while growing; the bacteria x_2 is growth-limited by the substrate s_2, and while it grows it produces the substrate s_1. The interaction among bacteria and substrates inside the chemostat has been illustrated in Fig. 2, and their rate of change (Δ) can be described by:

$$\begin{aligned}
&\text{nutrient}_1\ \Delta = \text{input}_1 - \text{uptake}_{x_1} + \text{production}_{x_2} - \text{outflow},\\
&\text{bacteria}_1\ \Delta = \text{growth}_{x_1} - \text{outflow},\\
&\text{nutrient}_2\ \Delta = \text{input}_2 - \text{uptake}_{x_2} + \text{production}_{x_1} - \text{outflow},\\
&\text{bacteria}_2\ \Delta = \text{growth}_{x_2} - \text{outflow},
\end{aligned} \tag{1}$$

where input_1=ds_1^{in} and input_2=ds_2^{in} are the inflow of growth-limiting substrates, the *outflow* terms indicate the flow of substances out of the tank. The substrate consumed by the bacteria x_1 and x_2 are $\text{uptake}_{x_1} = \frac{m_1 s_1 x_1}{\gamma_1(s_1+a_1)}$ and $\text{uptake}_{x_2} = \frac{m_2 s_2 x_2}{\gamma_2(s_2+a_2)}$, respectively; these are Monod functions, also known as Michaelis-Menten equations [9], where m_i, a_i and γ_i denote the maximum growth rate, half-saturation constant and

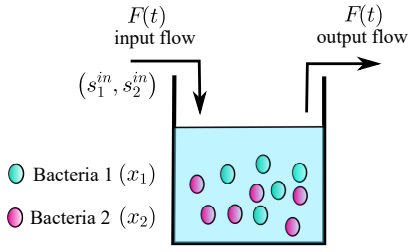

Fig. 1. Continuous stirred tank bioreactor with two bacteria.

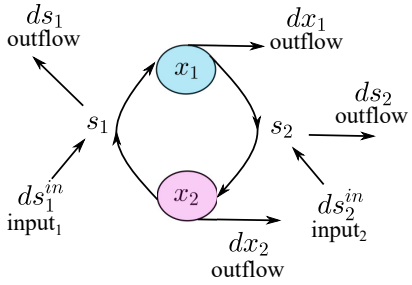

Fig. 2. Illustration of the bacteria and substrates interaction.

yield constant for the bacteria i, with $i\in\{1,2\}$, respectively. The yield constants are the mass relation between formed organism and consumed substrate, $\gamma_i=\frac{\text{mass of } x_i \text{ formed}}{\text{mass of } s_i \text{ consumed}}$. Bacterial growth is the product of substrate consumption and its yield constant, i.e., $\text{growth}_{x_1}=\frac{m_1 s_1 x_1}{s_1+a_1}$ and $\text{growth}_{x_2}=\frac{m_2 s_2 x_2}{s_2+a_2}$. The $\text{production}_{x_1}=\beta_1\left(\frac{m_1 s_1 x_1}{s_1+a_1}\right)$ term indicates the production of s_2 by the bacteria x_1 and $\text{production}_{x_2}=\beta_2\left(\frac{m_2 s_2 x_2}{s_2+a_2}\right)$ indicates the production of s_1 by the bacteria x_2, where $\beta_1>0$ and $\beta_2>0$. Combining the previous as indicated in (1) yields:

$$\begin{aligned}\dot{s}_1 &= ds_1^{in}-\tfrac{m_1 x_1 s_1}{\gamma_1(s_1+a_1)}+\beta_2\left(\tfrac{m_2 s_2 x_2}{s_2+a_2}\right)-ds_1,\\ \dot{s}_2 &= ds_2^{in}-\tfrac{m_2 x_2 s_2}{\gamma_2(s_2+a_2)}+\beta_1\left(\tfrac{m_1 s_1 x_1}{s_1+a_1}\right)-ds_2,\\ \dot{x}_1 &= \tfrac{m_1 s_1 x_1}{s_1+a_1}-dx_1,\quad \dot{x}_2=\tfrac{m_2 s_2 x_2}{s_2+a_2}-dx_2,\end{aligned}\tag{2}$$

Now, we proceed to study the properties of the model.

III. Model analysis

A. Positive invariance

The model solutions must be coherent; in our case the states correspond to concentrations; thus, they must be nonnegative. First, consider the bacteria trajectory at the border of the positive orthant, that is, $x_1{=}0$ and $x_2{=}0$ in (2); which yields $\dot{x}_1=0$ and $\dot{x}_2=0$. Therefore, if the bacteria concentrations were initialized with a nonnegative value their solution will be nonnegative, $x_1(0)\geq 0$ and $x_2(0)\geq 0$ implies $x_1(t)\geq 0$ and $x_2(t)\geq 0$, $\forall t\geq 0$. Now, if the substrates are $s_1{=}0$ and $s_2{=}0$ in (2) gives $\dot{s}_1{=}ds_1^{in}{+}\beta_2\left(\frac{m_2 s_2 x_2}{s_2+a_2}\right)$ and $\dot{s}_2{=}ds_2^{in}{+}\beta_1\left(\frac{m_1 s_1 x_1}{s_1+a_1}\right)$; so, if they are nonnegative their solution is nonnegative, $s_1(0)\geq 0$ and $s_2(0)\geq 0$ implies $s_1(t){\geq}0$ and $s_2(t){\geq}0$, $\forall t\geq 0$.

B. Model reduction

Chemostat systems must satisfy the mass conservation principle, and a common approach is to reduce the order of the model [10], it can be either to avoid numerical errors in simulation or to simplify its analysis [11]. First define $\hat{x}=\begin{bmatrix}s_1 & x_1 & s_2 & x_2\end{bmatrix}^T$, and rewrite (2) in the form $\dot{\hat{x}}{=}Kv(\hat{x}){+}\hat{x}_{io}$:

$$\underbrace{\begin{bmatrix}\dot{s}_1\\ \dot{x}_1\\ \dot{s}_2\\ \dot{x}_2\end{bmatrix}}_{\dot{\hat{x}}}=\underbrace{\begin{bmatrix}-\frac{1}{\gamma_1} & \beta_2\\ 1 & 0\\ \beta_1 & -\frac{1}{\gamma_2}\\ 0 & 1\end{bmatrix}}_{K}\underbrace{\begin{bmatrix}\frac{m_1 x_1 s_1}{s_1+a_1}\\ \frac{m_2 x_2 s_2}{s_2+a_2}\end{bmatrix}}_{v(\hat{x})}+\underbrace{\begin{bmatrix}d\left(s_1^{in}-s_1\right)\\ -dx_1\\ d\left(s_2^{in}-s_2\right)\\ -dx_2\end{bmatrix}}_{\hat{x}_{io}},\tag{3}$$

where K is the stoichiometric matrix, with $\text{rank}(K){=}m{<}n$, and n is the number of states. Then, find a matrix N in the left-kernel of K, i.e., $\exists N\neq 0 : NK=0$; a possible choice is $N{=}\begin{bmatrix}\gamma_1 & 1 & 0 & -\gamma_1\beta_2\\ 0 & -\gamma_2\beta_1 & \gamma_2 & 1\end{bmatrix}$, and define the variables $z{=}N\hat{x}$:

$$z_1{=}\gamma_1 s_1{+}x_1{-}\beta_2\gamma_1 x_2,\quad z_2{=}x_2{+}\gamma_2 s_2{-}\beta_1\gamma_2 x_1.\tag{4}$$

Their dynamics are $\dot{z}=N\dot{\hat{x}}=NKv(\hat{x}){+}N\hat{x}_{io}=N\hat{x}_{io}$, it yields to $\dot{z}_1=d\left(\gamma_1\left(s_1^{in}{+}\beta_2 x_2{-}s_1\right){-}x_1\right)$ and $\dot{z}_2=d\left(\gamma_2\left(s_2^{in}{+}\beta_1 x_1{-}s_2\right){-}x_2\right)$, substitute $\beta_2\gamma_1 x_2{=}x_1{-}z_1{+}\gamma_1 s_1$ and $\beta_1\gamma_2 x_1{=}x_2{-}z_2{+}\gamma_2 s_2$, to get $\begin{bmatrix}\dot{z}_1\\ \dot{z}_2\end{bmatrix}{=}\begin{bmatrix}-d & 0\\ 0 & -d\end{bmatrix}\begin{bmatrix}z_1\\ z_2\end{bmatrix}{+}\begin{bmatrix}d\gamma_1 s_1^{in}\\ d\gamma_2 s_2^{in}\end{bmatrix}$, then, rewrite the substrates as $s_1=\beta_2 x_2+\frac{z_1-x_1}{\gamma_1}\geq 0$ and $s_2=\beta_1 x_1+\frac{z_2-x_2}{\gamma_2}\geq 0$ in (2) to express the system as

$$\begin{aligned}\dot{x}_1&=\left(\frac{m_1\left(\beta_2 x_2+\frac{z_1-x_1}{\gamma_1}\right)}{\beta_2 x_2+\frac{z_1-x_1}{\gamma_1}+a_1}-d\right)x_1,\quad \dot{z}_1=-dz_1+d\gamma_1 s_1^{in},\\ \dot{x}_2&=\left(\frac{m_2\left(\beta_1 x_1+\frac{z_2-x_2}{\gamma_2}\right)}{\beta_1 x_1+\frac{z_2-x_2}{\gamma_2}+a_2}-d\right)x_2,\quad \dot{z}_2=-dz_2+d\gamma_2 s_2^{in}.\end{aligned}\tag{5}$$

Notice that if $t_0{=}0$, $z_1(0){=}x_1(0){+}\gamma_1 s_1(0){-}\beta_2\gamma_1 x_2(0)$ and $z_2(0){=}x_2(0){+}\gamma_2 s_2(0){-}\beta_1\gamma_2 x_1(0)$; then, we can integrate $z_i(t)$, with $i\in\{1,2\}$, as $z_i(t){=}e^{-dt}z_i(0){+}\gamma_i s_i^{in}\left(1{-}e^{-dt}\right)$. Thus, if $d\neq 0$ any trajectory has an unique equilibria at $z_1^*{=}\gamma_1 s_1^{in}$ and $z_2^*{=}\gamma_2 s_2^{in}$. After the two pseudo first integral described by z_1 and z_2 in (5) have converged to their equilibria we can substitute $z_1{=}\gamma_1 s_1^{in}$ and $z_2{=}\gamma_2 s_2^{in}$ in (5) to obtain

$$\dot{x}_1{=}\left(\frac{m_1\left(\beta_2 x_2{-}\frac{x_1}{\gamma_1}{+}s_1^{in}\right)}{\beta_2 x_2{-}\frac{x_1}{\gamma_1}{+}s_1^{in}{+}a_1}{-}d\right)x_1,\ \dot{x}_2{=}\left(\frac{m_2\left(\beta_1 x_1{-}\frac{x_2}{\gamma_2}{+}s_2^{in}\right)}{\beta_1 x_1{-}\frac{x_2}{\gamma_2}{+}s_2^{in}{+}a_2}{-}d\right)x_2,\tag{6}$$

which describe the chemostat behavior after an initial transient. In the next subsection we will analyse their equilibrium points.

C. Equilibrium points

This subsection is dedicated to obtain the equilibrium points of the reduced order model. For notation simplification consider $\xi_1{=}m_1{-}d$, $\xi_2{=}m_2{-}d$, $\zeta_1{=}\xi_1 s_1^{in}{-}da_1$, $\zeta_2{=}\xi_2 s_2^{in}{-}da_2$, and $\xi_3{=}1{-}\gamma_1\gamma_2\beta_1\beta_2$. The equilibrium points are at the intersection of the nullclines (6); these are $0{=}\left(\frac{m_1\left(\beta_2 x_2{-}\frac{x_1}{\gamma_1}{+}s_1^{in}\right)}{\beta_2 x_2{-}\frac{x_1}{\gamma_1}{+}s_1^{in}{+}a_1}{-}d\right)x_1$, and $0{=}\left(\frac{m_2\left(\beta_1 x_1{-}\frac{x_2}{\gamma_2}{+}s_2^{in}\right)}{\beta_1 x_1{-}\frac{x_2}{\gamma_2}{+}s_2^{in}{+}a_2}{-}d\right)x_2$; the intersections occur at:

1) The trivial case $(x_1^\star=0, x_2^\star=0)$, known as washout.
2) The case $(x_1^\star\neq 0, x_2^\star{=}0)$ yields to $x_1^\star{=}\gamma_1\left(s_1^{in}-\frac{da_1}{m_1-d}\right)$, it exists if $d<\frac{m_1 s_1^{in}}{s_1^{in}+a_1}$ holds.
3) The case $(x_1^\star{=}0, x_2^\star\neq 0)$ it gives $x_2^\star{=}\gamma_2\left(s_2^{in}-\frac{da_2}{m_2-d}\right)$, and exists if $d<\frac{m_2 s_2^{in}}{s_2^{in}+a_2}$ holds.
4) The interior equilibrium $(x_1^\star\neq 0, x_2^\star\neq 0)$ is located at

$$\begin{aligned}x_1^\star&=\tfrac{\gamma_1}{\xi_3}\left(s_1^{in}+\beta_2\gamma_2 s_2^{in}-d\left(\tfrac{a_1}{m_1-d}+\tfrac{a_2\beta_2\gamma_2}{m_2-d}\right)\right),\\ x_2^\star&=\tfrac{\gamma_2}{\xi_3}\left(s_2^{in}+\beta_1\gamma_1 s_1^{in}-d\left(\tfrac{a_2}{m_2-d}+\tfrac{a_1\beta_1\gamma_1}{m_1-d}\right)\right),\end{aligned}$$

it will exists if $\gamma_1\gamma_2\beta_1\beta_2 < 1$ and $d<\min\left(m_1, m_2, \frac{-\omega_{11}\pm\sqrt{\omega_{11}^2-4\omega_{12}}}{2}, \frac{-\omega_{21}\pm\sqrt{\omega_{21}^2-4\omega_{22}}}{2}\right)$,

hold, with $\omega_{11} = -\frac{(m_1+m_2)\left(s_1^{in}+\beta_2\gamma_2 s_2^{in}\right)+a_1 m_2+a_2 m_1\beta_2\gamma_2}{a_1+s_1^{in}+\left(a_2+s_2^{in}\right)\beta_2\gamma_2}$,
$\omega_{21} = -\frac{(m_1+m_2)\left(s_2^{in}+\beta_1\gamma_1 s_1^{in}\right)+a_2 m_1+a_1 m_2\beta_1\gamma_1}{a_2+s_2^{in}+\left(a_1+s_1^{in}\right)\beta_1\gamma_1}$,
$\omega_{12}=\frac{m_1 m_2\left(s_1^{in}+\beta_2\gamma_2 s_2^{in}\right)}{a_1+s_1^{in}+\left(a_2+s_2^{in}\right)\beta_2\gamma_2}$, and $\omega_{22}=\frac{m_1 m_2\left(s_2^{in}+\beta_1\gamma_1 s_1^{in}\right)}{a_2+s_2^{in}+\left(a_1+s_1^{in}\right)\beta_1\gamma_1}$.
From the previous we can see that the interior equilibrium point (persistence case) might exist even if one of the input substrates is equals to zero, $(s_1^{in}=0, s_2^{in}=0)$. Moreover, the bacteria concentration higher in the case of coexistence compared to their isolation value [5]. The steady-state for $d=0$ is out of the scope for this manuscript because it does not corresponds to a continuous bioreactor, but to a batch culture. Each equilibrium point of the reduced model (6) corresponds to an unique point of the original (2) obtained by substituting $z_1^\star$, $z_2^\star$, $x_1^\star$ and $x_2^\star$ into $s_1^\star=\beta_2 x_2^\star+\frac{z_1^\star-x_1^\star}{\gamma_1}$ and $s_2^\star=\beta_1 x_1^\star+\frac{z_2^\star-x_2^\star}{\gamma_2}$.

D. Local stability of the bacteria concentration

Now we study the local stability of the equilibrium points. It can be done either by computing a linearization of the reduced order model (6) at the equilibrium points (Jacobian matrix) and examining its eigenvalues; or since (6) is a second order, an alternative is verifying that its trace and determinant are negative and positive, respectively. The Jacobian matrix is

$$J|_{x_1^\star,x_2^\star}=\begin{bmatrix}\mu_1-d-\left(\frac{x_1^\star}{\gamma_1}\right)\mu_1^{'} & \beta_2 x_1^\star\mu_1^{'}\\ \beta_1 x_2^\star\mu_2^{'} & \mu_2-d-\left(\frac{x_2^\star}{\gamma_2}\right)\mu_2^{'}\end{bmatrix}, \quad (7)$$

where $\mu_1 = \frac{m_1\left(\beta_2 x_2^\star-\frac{x_1^\star}{\gamma_1}+s_1^{in}\right)}{\beta_2 x_2^\star-\frac{x_1^\star}{\gamma_1}+s_1^{in}+a_1}$, $\mu_2 = \frac{m_2\left(\beta_1 x_1^\star-\frac{x_2^\star}{\gamma_2}+s_2^{in}\right)}{\beta_1 x_1^\star-\frac{x_2^\star}{\gamma_2}+s_2^{in}+a_2}$, $\mu_1^{'} = \frac{a_1 m_1}{\left(a_1-\frac{x_1^\star}{\gamma_1}+s_1^{in}+\beta_2 x_2^\star\right)^2}$ and $\mu_2^{'} = \frac{a_2 m_2}{\left(a_2-\frac{x_2^\star}{\gamma_1}+s_2^{in}+\beta_1 x_1^\star\right)^2}$.
The corresponding values for each case are:

1) The eigenvalues of the Jacobian matrix for the washout case are $\sigma_1=\frac{\zeta_1}{a_1+s_1^{in}}$ and $\sigma_2=\frac{\zeta_2}{a_2+s_2^{in}}$. Therefore, it is stable if $d>\max\left(\frac{m_1 s_1^{in}}{s_1^{in}+a_1}, \frac{m_2 s_2^{in}}{s_2^{in}+a_2}\right)$ holds.
2) In the case $(x_1^\star\neq 0, x_2^\star=0)$ the trace and determinant are $J_{11}+J_{22}$ and $J_{11}J_{22}$, respectively, with $J_{11}=-\frac{\xi_1\zeta_1}{a_1 m_1}$ and $J_{22}=\frac{m_2\left(s_2^{in}+\frac{\beta_1\gamma_1\zeta_1}{\xi_1}\right)}{a_2+s_2^{in}+\frac{\beta_1\gamma_1\zeta_1}{\xi_1}}-d$. Thus, J_{11} and J_{22} are negative if $d<\min\left(\frac{m_1 s_1^{in}}{s_1^{in}+a_1}, \frac{-\omega_{21}\pm\sqrt{\omega_{21}^2-4\omega_{22}}}{2}\right)$ holds.
3) For the case $(x_1^\star=0, x_2^\star\neq 0)$ the diagonal terms are $J_{11}=\frac{m_1\left(s_1^{in}+\frac{\beta_2\gamma_2\zeta_2}{\xi_2}\right)}{a_1+s_1^{in}+\frac{\beta_2\gamma_2\zeta_2}{m_2-d}}-d$ and $J_{22}=\frac{-\xi_2\zeta_2}{a_2 m_2}$; both are negative if $d<\min\left(\frac{m_2 s_2^{in}}{s_2^{in}+a_2}, \frac{-\omega_{11}\pm\sqrt{\omega_{11}^2-4\omega_{12}}}{2}\right)$ holds.
4) In the persistence case $(x_1^\star\neq 0, x_2^\star\neq 0)$ it holds that $\mu_1-d=0$ and $\mu_2-d=0$. From the Jacobian (7) we get $\det(J)=\mu_1^{'}\mu_2^{'}\left(\left(\frac{1}{\gamma_1\gamma_2}-\beta_1\beta_2\right)x_1^\star x_2^\star\right)$ and $Tr(J)=-\frac{x_1^\star}{\gamma_1}\mu_1^{'}-\frac{x_2^\star}{\gamma_2}\mu_2^{'}$. Thus, it is stable if $\gamma_1\gamma_2\beta_1\beta_2<1$ holds.

E. Global stability

Now we can analyse the global behavior of the system's solutions for the coexistence case. First, assume that the conditions for the existence of this point are met, $\gamma_1\gamma_2\beta_1\beta_2<1$ and $d<\min\left(m_1, m_2, \frac{-\omega_{11}\pm\sqrt{\omega_{11}^2-4\omega_{12}}}{2}, \frac{-\omega_{21}\pm\sqrt{\omega_{21}^2-4\omega_{22}}}{2}\right)$. Then, consider as initial conditions the points p^i in Fig. 3, where $i\in\{1,2,3,4\}$ and estimate the direction for each trajectory:

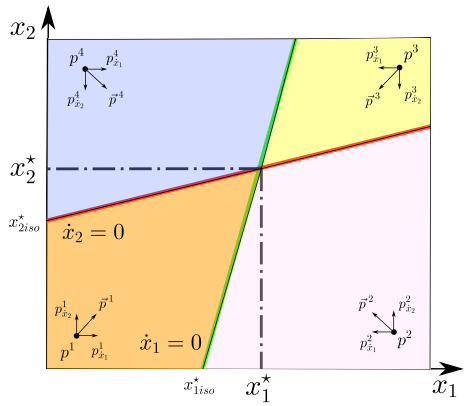

Fig. 3. Direction of the trajectories $\vec{p}^i$ for possible initial conditions p^i, nullclines $(\dot{x}_1=0, \dot{x}_2=0)$, isolated equilibria $\left(x_{1iso}^\star, x_{2iso}^\star\right)$ and intersection.

1) In the case of p^1, if the bacteria concentrations x_1 and x_2 are both small enough, respectively, from (6) it follows that $\dot{x}_1>0$ and $\dot{x}_2>0$ holds.
2) If we go from the point p^1 to the point p^2, we have to cross the nullcline $\dot{x}_1=0$, so there must be a change of sign on the time derivative $\dot{x}_1$, it yields to $\dot{x}_1<0$ and $\dot{x}_2>0$, the direction of the trajectory is indicated by $\vec{p}^{\,2}$.
3) If we move from the point p^1 to the point p^3 we must cross two nullclines to get there ($\dot{x}_1=0$ and $\dot{x}_2=0$); therefore, the sign of both time derivatives changes to $\dot{x}_1<0$ and $\dot{x}_2<0$, and the trajectory is indicated by $\vec{p}^{\,3}$.
4) In order to go from p^1 to p^4 we must cross the nullcline corresponding to $\dot{x}_2=0$, therefore, there is a change of sign on $\dot{x}_2$, which produces $\dot{x}_1>0$ and $\dot{x}_2<0$ as indicated by the direction of the trajectory in $\vec{p}^{\,4}$.

Notice that the nullcline $\dot{x}_1=0$ can only be crossed by means of $\dot{x}_2$ and vice-versa. Thus, any trajectory on the regions where the points p^2 or p^4 are located will be pushed to the regions of the points p^1 or p^3; the latter regions are invariant, that is, trajectories can not escape from them. After that the solution can only head towards the coexistence equilibrium. Then, we can conclude that the interior equilibrium is globally stable.

We have proven global stability for the reduced system in dimension two. Global stability for the full system (5) is easy to deduce by classical arguments of asymptotically autonomous systems. Considering the linear dynamics of the equations for (z_1, z_2), we can for example apply the Convergence Theorem of Appendix F in [9]. Moreover, we remark that the system (5) is a monotone and cooperative system (see section V); therefore, it has strong properties of convergence. It is easy to see that we would be able to study the same mutualism system in the case of $N-$bacteria forming a closed-loop to feed each other, using these properties of stability of monotone systems. This cannot be detailed here due to lack of space.

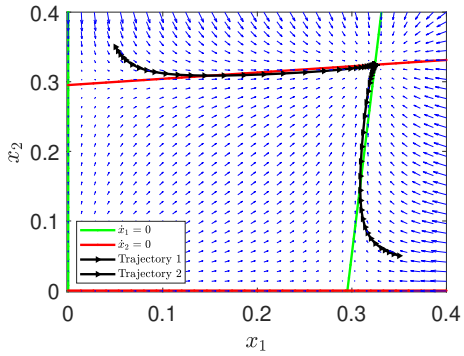

Fig. 4. Phase portrait of the bacteria $(x_1 - x_2)$ for Example 1, nullclines for $\dot{x}_1 = 0$ and $\dot{x}_2 = 0$ are indicated in green and red, respectively. Trajectories from simulation with initial conditions $(0.05, 0.35)$ and $(0.35, 0.05)$.

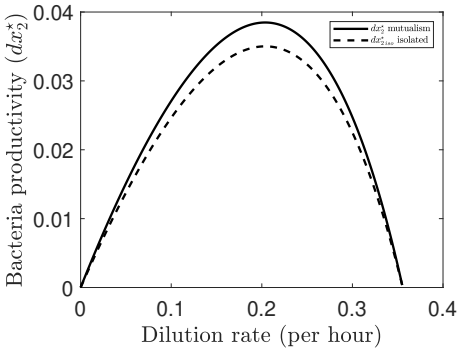

Fig. 5. Productivity of x_2 in mutualism and isolated cases.

Example 1. *Consider the parameters* $s_i^{in} = 0.4$ *(g/l),* $m_i = 0.8$ *(per hour),* $a_i = 0.5$ *(g/l),* $\gamma_i = 0.75$, $\beta_i = 0.12$ *and* $d = 0.01$ *(per hour), with* $i \in \{1, 2\}$. *The phase-portrait obtained is in Fig. 4. According to subsections III-D and III-D the interior equilibrium is* $(x_1^\star, x_2^\star) = (0.3245, 0.3245)$, *while the isolated equilibria are* $(x_{1iso}^\star, x_{2iso}^\star) = (0.2953, 0.2953)$; *it illustrates that concentrations in coexistence are higher than in isolation.*

IV. Steady-state optimization

Here we find the optimal dilution rate and metabolite production term to maximize the productivity of the chemostat.

A. Optimal dilution rate

First, let us define the bacterial productivity as the product of bacteria concentration at steady-state and the dilution rate of the chemostat; and we would like to find an optimal value for the dilution rate that maximizes this bacterial productivity

$$Y(d) = dx_2^\star = \frac{\gamma_1}{\xi_3}\left(\frac{p_1(d)}{p_2(d)}\right) = \frac{\gamma_1}{\xi_3}\left(\frac{\delta_1 d^3 + \delta_2 d^2 + \delta_3 d}{d^2 - d(m_1+m_2) + m_1 m_2}\right), \quad (8)$$

with $\delta_1 = a_2 + s_2^{in} + \left(a_1 + s_1^{in}\right)\beta_1\gamma_1$, $\delta_2 = -(m_1+m_2)\left(s_2^{in} + \beta_1\gamma_1 s_1^{in}\right) - a_2 m_1 - a_1\beta_1\gamma_1 m_2$, and $\delta_3 = m_1 m_2\left(s_2^{in} + \beta_1\gamma_1 s_1^{in}\right)$. The critical points of (8) can be obtained by solving $\frac{\partial Y(d)}{\partial d} = \frac{\gamma_1\left(p_2(d)\frac{\partial p_1(d)}{\partial d} - p_1(d)\frac{\partial p_2(d)}{\partial d}\right)}{\xi_3 p_2^2(d)} = \frac{\delta_1 p_3(d)}{\xi_3 p_2^2(d)} = 0$ for d, where $\frac{\partial p_1(d)}{\partial d} = 3\delta_1 d^2 + 2\delta_2 d + \delta_3$, $\frac{\partial p_2(d)}{\partial d} = 2d - m_1 - m_2$, $p_3(d) = d^4 + \Delta_1 d^3 + \Delta_2 d^2 + \Delta_3 d + \Delta_4$, $\Delta_1 = -2(m_1+m_2)$, $\Delta_2 = -\frac{(\delta_3 + \delta_2(m_1+m_2) - 3\delta_1 m_1 m_2)}{\delta_1}$, $\Delta_3 = \frac{2\delta_2 m_1 m_2}{\delta_1}$ and $\Delta_4 = \frac{\delta_3 m_1 m_2}{\delta_1}$. This critical dilution rate (d_c) is computed via numerical methods. Then, we can evaluate the second partial derivative

$$\frac{\partial Y(d)}{\partial^2 d} = \frac{\gamma_1\delta_1\left(p_2^2(d)\frac{\partial p_3(d)}{\partial d} - p_3(d)\frac{\partial p_2^2(d)}{\partial d}\right)}{\xi_3 p_2^4(d)} = \frac{\gamma_1\delta_1\left(\frac{\partial p_3(d)}{\partial d}\right)}{\xi_3 p_2^2(d)}, \quad (9)$$

to determine if d_c corresponds to a local maximum $\left(\frac{\partial Y(d_c)}{\partial^2 d} < 0\right)$ of (8), the sign of $\frac{\partial Y(d_c)}{\partial^2 d}$ is determined by $\frac{\partial p_3(d)}{\partial d} = 4d^3 + 3\Delta_1 d^2 + 2\Delta_2 d + \Delta_3$. Finally, we must verify that d_c satisfies the coexistence conditions in subsection III-C.

Example 2 (Optimal dilution)**.** *Consider the previous chemostat values and compute the solutions for* $p_3(d)$, *the critical dilution rates obtained were* $d_c = [0.2037, 0.8, 1.3963]$. *Only* $d_c = 0.2037$ *satisfies the conditions for coexistence. Moreover, evaluating this critical dilution rate gives* $\frac{\partial p_3(d_c)}{\partial d} = -0.4240$. *As indicated,* d_c *corresponds to a local maximum. The bacterial productivity function* $Y(d)$ *for the mutualism and isolated cases within an operational range* $d \in [0.00001, 0.355]$ *are shown in Fig. 5 as well as the optimal dilution rate computed. As foreseen in Fig. 5 the mutualistic case is more advantageous than the isolated, since higher concentrations can be achieved.*

B. Optimal substrate production

Optogenetic techniques [12] allow us to control the metabolite production in bacteria. Thus, now we assume that our variable of control is the metabolite production of bacteria x_1 and we want to find an optimal β_1 to maximize $Y(\beta_1) = dx_2^\star = \frac{p_1(\beta_1)}{p_2(\beta_1)}$, with $p_1(\beta_1) = d\gamma_1 s_2^{in} - \frac{d^2\gamma_1^2 a_2}{m_2 - d} + \beta_1 d\gamma_1^2\left(s_1^{in} - \frac{a_1}{m_1 - d}\right)$ and $p_2(\beta_1) = 1 - \beta_1\beta_2\gamma_1\gamma_2$. Computing $\frac{\partial Y(\beta_1)}{\partial \beta_1} = \frac{d\gamma_1^2\left(s_1^{in} - \frac{a_1}{m_1 - d} + \beta_2\gamma_2\left(s_2^{in} - \frac{a_2 d\gamma_1}{m_2 - d}\right)\right)}{(1 - \beta_1\beta_2\gamma_1\gamma_2)^2} = 0$, we can see that the sign of this partial derivative is constant $\frac{\partial Y(\beta_1)}{\partial \beta_1} > 0$. Thus, the maximum of the cost function $Y(\beta_1)$ is determined by the maximum value of β_1 that we can provide.

V. Interval detector

We assume that the initial conditions of the system $X(0) = \begin{bmatrix} x_1(0) & x_2(0) & z_1(0) & z_2(0) \end{bmatrix}^T$ are unknown and bounded by maximum and minimum known values, $\bar{X}(0) \geq X(0) \geq \underline{X}(0)$. A system is said observable when its states can be reconstructed from its output. Similarly, a system is detectable when unobservable states are stable. We will employ the concept of detectability, as well as other model properties to design an interval detector that estimates upper and lower bounds of the states. These bounds can be used to estimate variables of interest such as bacterial productivity $(dx_2^\star)$. The system (5) is cooperative, which means that the off-diagonal terms of its Jacobian matrix $(\mathcal{J})$ are nonnegative, this matrix has the form $\mathcal{J} = \begin{bmatrix} - & \mathcal{J}_{12} & \mathcal{J}_{13} & 0 \\ \mathcal{J}_{21} & - & 0 & \mathcal{J}_{24} \\ 0 & 0 & - & 0 \\ 0 & 0 & 0 & - \end{bmatrix}$, where $\mathcal{J}_{12} = \frac{a_1\beta_2\gamma_1^2 m_1 x_1}{(z_1 - x_1 + \gamma_1(a_1 + \beta_2 x_2))^2}$,

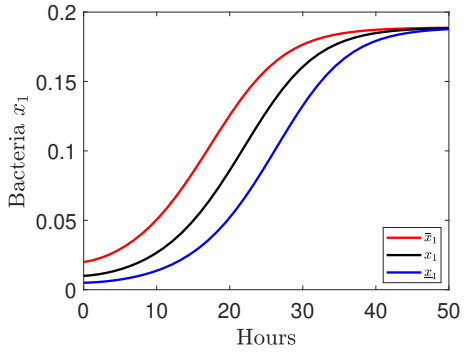

(a) Bacteria x_1 and its admissible trajectories.

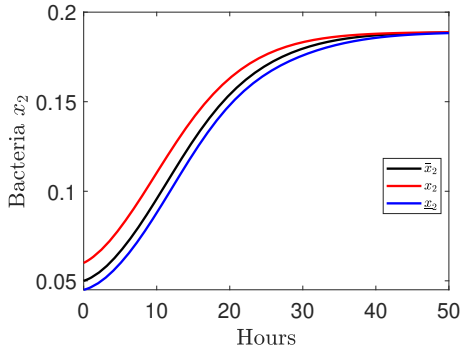

(b) Bacteria x_2 and its admissible trajectories.

Fig. 6. Unmeasured bacteria (x_1, x_2) and their estimation.

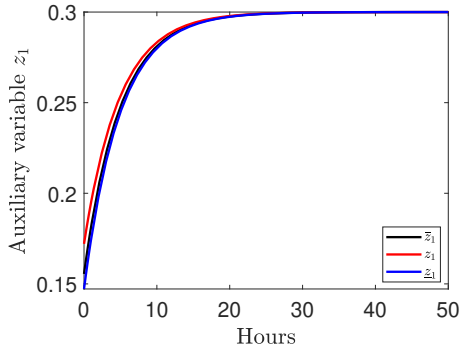

(a) Variable z_1 and its admissible trajectories.

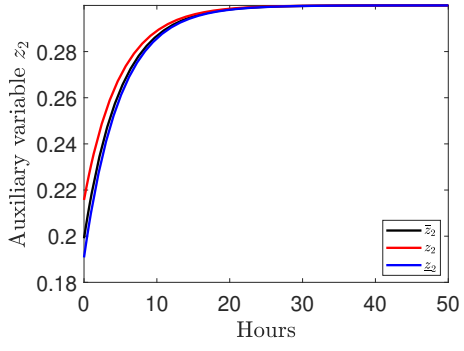

(b) Variable z_2 and its admissible trajectories.

Fig. 7. Unmeasured states (z_1, z_2) and their estimation.

$\mathcal{J}_{13} = \frac{a_1\gamma_1 m_1 x_1}{(z_1 - x_1 + \gamma_1(a_1+\beta_2 x_2))^2}$, $\mathcal{J}_{21} = \frac{a_2\beta_1\gamma_2^2 m_2 x_2}{(z_2 - x_2 + \gamma_2(a_2+\beta_1 x_1))^2}$ and $\mathcal{J}_{24} = \frac{a_2\gamma_2 m_2 x_2}{(z_2 - x_2 + \gamma_2(a_2+\beta_1 x_1))^2}$. Cooperative systems have the property of preserving their order [9], $\bar{X}(t) \geq X(t) \geq \underline{X}(t)$, holds $\forall t \geq 0$, when properly initialized, $\bar{X}(0) \geq X(0) \geq \underline{X}(0)$. Thus, we can construct the interval asymptotic detector:

$$\begin{aligned} \dot{\bar{x}}_i &= \left(\frac{m_i\left(\beta_j \bar{x}_j + \frac{\bar{z}_i - \bar{x}_i}{\gamma_i}\right)}{\beta_j \bar{x}_j + \frac{\bar{z}_i - \bar{x}_i}{\gamma_i} + a_i} - d \right) \bar{x}_i,\ \dot{\bar{z}}_i = -d\bar{z}_i + d\gamma_i s_i^{in}, \\ \dot{\underline{x}}_i &= \left(\frac{m_i\left(\beta_j \underline{x}_j + \frac{\underline{z}_i - \underline{x}_i}{\gamma_i}\right)}{\beta_j \underline{x}_j + \frac{\underline{z}_i - \underline{x}_i}{\gamma_i} + a_i} - d \right) \underline{x}_i,\ \dot{\underline{z}}_i = -d\underline{z}_i + d\gamma_i s_i^{in}, \end{aligned} \tag{10}$$

with $(i,j) \in \{1,2,\}$, $i \neq j$, where $(\bar{x}_i, \bar{z}_i)$ and $(\underline{x}_i, \underline{z}_i)$ corresponds to the upper and lower estimations of the bacteria concentration and auxiliary variables, respectively. We can obtain an asymptotic estimation of the states from it. In Fig. 6 the states time evolution and their bounds is shown, with a dilution rate $d = 0.2037$, the initial conditions for the system, upper and lower estimations were $X(0) = \begin{bmatrix}0.01 & 0.05 & 0.1555 & 0.1991\end{bmatrix}^T$, $\bar{X}(0) = \begin{bmatrix}0.02 & 0.06 & 0.1721 & 0.2157\end{bmatrix}^T$ and $\underline{X}(0) = \begin{bmatrix}0.005 & 0.045 & 0.1472 & 0.1908\end{bmatrix}^T$, respectively.

Since $\underline{x}_2 \leq x_2 \leq \bar{x}_2$ holds, we can compute upper and lower bounds of the productivity as $d\underline{x}_2 \leq dx_2 \leq d\bar{x}_2$; we will employ it to optimize the dilution rate in the following section.

VI. Online dilution optimization

In this section we assume that the dilution rate is periodic, to our knowledge, an analytical solution for a periodic dilution rate it not available. Thus, here we will present different optimization strategies using the interval detector. Our approach is inspired by the extreme seeking algorithm [13].

A. Average optimization

Consider a periodic dilution rate $d(t) = a(1 + b\sin(\omega t))$, where $a > 0$, $0 < b < 1$ and $\omega > 0$. Then, assume the lower estimation of the bacteria is available, $\underline{x}_2(t)$ and we want to maximize the average of the estimated productivity $Avg(d(t)\,\underline{x}_2(t))$ measured over a period $T = \frac{1}{f}$, $\omega = 2\pi f$, with a sufficiently large initial averaging time (t_0), that is, the system trajectories are near to a periodic regime, then, our objective function is $Avg(d\underline{x}_2) = \frac{1}{T}\int_{t_0}^{t_0+T} d(t)\,\underline{x}_2(t)\,dt$. Since the signal order is preserved, the system and the interval detector converge to the same periodic regime; so, it follows that $Avg(d\underline{x}_2) \leq Avg(dx_2) \leq Avg(d\bar{x}_2)$, holds.

Example 3. *The parameters considered are $a = 0.01$, $f = 0.005$ Hz and $b = 0.5$, the evolution of the productivity is shown in Fig. 8a. The averages obtained considering $a \in (0.001, 0.355)$ are in Fig. 8b (black line). Only $Avg(d\underline{x}_2)$ is shown because the states and the estimated are in a periodic regime, so the signals average are overlapped.*

B. Heuristic optimization

Here we present an heuristic method to optimize the dilution rate. Consider a periodic dilution rate $d(t) = a_i(1 + b\sin(\omega t))$, where $a_i > 0$, $0 \leq b \leq 1$, $\omega > 0$ and follow this algorithm:

1) First, provide positive initial values for a_0 and ϵ_0, then, measure the T-average bacterial production.

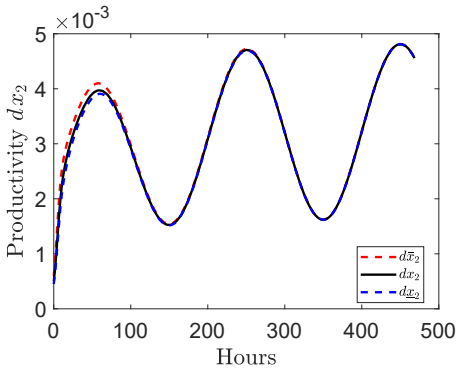

(a) Instantaneous productivity (black line), upper and lower bounds (red and blue dashed lines, respetively).

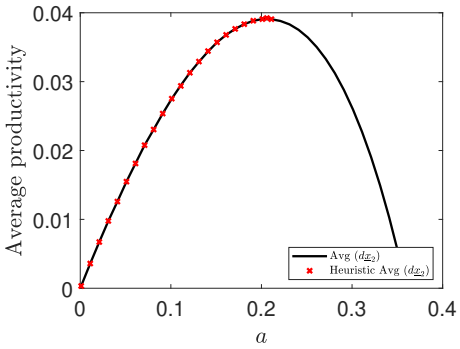

(b) Average productivity for $a \in (0.001, 0.355)$ with approach in subsection VI-A (black line) and with the heuristic approach in subsection VI-B (red crosses).

Fig. 8. Instantaneous and average productivity in simulation.

2) Compute a provisional a_i value as $a_p = |a_i + \epsilon_k|$, where $|\cdot|$ takes the absolute value of the argument; estimate the T-average for a_p, and if the T-average is higher than its value for a_i, then, update $a_{i+1} = a_p$ and repeat this step. Otherwise, compute a new ϵ_k as $\epsilon_k = \frac{-\epsilon_k}{2}$ and repeat.
3) The algorithm can finish after a number of predefined iterations $(i_{\max}, k_{\max})$ or when the difference between average productivity measured is below a threshold.

Example 4. *Consider $a_0 = 0.005$ and $\epsilon_0 = 0.01$. The algorithm begins at a_0, computes the T-average and compares it with the T-average for $a_p = a_0 + \epsilon_0$. Since the average is higher, it updates $a_{i+1} = a_p$, and repeats until finding a lower productivity; then, updates $\epsilon_1 = -\frac{\epsilon_0}{2}$, computes a new a_{i+1} and measures its T-average until $i_{\max} = 24$. The final values were $a_{24} = 0.201$ and $\epsilon_1 = -0.005$. The results are illustrated in Fig. 8b (red crosses), the other parameters remain the same.*

VII. Conclusion

The mathematical model for two bacteria growing under cross-feeding interaction was presented, its steady-state and stability were studied. Through an analysis of the vector field trajectories we could conclude that when the interior equilibrium (persistence case) exists it is globally stable. As in other mutualism cases the bacteria concentration in coexistence is higher than isolation. The optimization of biomass production for a bacteria of interest at steady-state was carried out.

Also, an interval detector was designed to compute upper and lower bounds of the trajectories. Here we assumed unknown initial conditions with known bounds and no measurements of the variables to estimate were required. The designed interval detector was employed to estimate the chemostat productivity, then, algorithms to optimize this productivity were presented. One of them based on the extremum seeking algorithm was adapted to periodic dilution rates, it is robust since is always looking for optimal values in a neighbourhood.

For the future of this work we can consider mutualism appearing in different scenarios such as algae and bacteria, that would require different models (like Droop [14] or Geider [15] models), but the analysis and optimization methods could be similar to the ones in this manuscript. Finally, it might be convenient improve the dilution rate update policy to take into account the signals provided by the interval detector. Additionally, we can consider uncertainties in the model parameters and take advantage of the Monod functions structure to build an interval detector to estimate bounds of the unmeasured states.

References

[1] L. Margulis, "Symbiosis and evolution," *Scientific American*, vol. 225, no. 2, pp. 48–61, 1971.
[2] A. M. Dean, "A simple model of mutualism," *The American Naturalist*, vol. 121, no. 3, pp. 409–417, 1983.
[3] S. Vet, S. de Buyl, K. Faust, J. Danckaert, D. Gonze, and L. Gelens, "Bistability in a system of two species interacting through mutualism as well as competition: Chemostat vs. lotka-volterra equations," *PloS one*, vol. 13, no. 6, p. e0197462, 2018.
[4] T. Sari, M. El Hajji, and J. Harmand, "The mathematical analysis of a syntrophic relationship between two microbial species in a chemostat," *Mathematical Biosciences and Engineering*, vol. 9, no. 3, pp. p–627, 2012.
[5] J. D. Murray, "Continuous models for interacting populations," in *Mathematical Biology*. Springer, 1993, pp. 63–94.
[6] N. W. Smith, P. R. Shorten, E. Altermann, N. C. Roy, and W. C. McNabb, "The classification and evolution of bacterial cross-feeding," *Frontiers in Ecology and Evolution*, vol. 7, p. 153, 2019.
[7] J. C. Moore, "The influence of microarthropods on symbiotic and non-symbiotic mutualism in detrital-based below-ground food webs," *Agriculture, ecosystems & environment*, vol. 24, no. 1-3, pp. 147–159, 1988.
[8] F. Abiusi, R. H. Wijffels, and M. Janssen, "Doubling of microalgae productivity by oxygen balanced mixotrophy," *ACS Sustainable Chemistry & Engineering*, vol. 8, no. 15, pp. 6065–6074, 2020.
[9] H. L. Smith and P. Waltman, *The theory of the chemostat: dynamics of microbial competition*. Cambridge university press, 1995, vol. 13.
[10] P. Benner and T. Stykel, "Model order reduction for differential-algebraic equations: a survey," in *Surveys in Differential-Algebraic Equations IV*. Springer, 2017, pp. 107–160.
[11] K. V. Waller and P. M. Makila, "Chemical reaction invariants and variants and their use in reactor modeling, simulation, and control," *Industrial & Engineering Chemistry Process Design and Development*, vol. 20, no. 1, pp. 1–11, 1981.
[12] K. Deisseroth, "Optogenetics," *Nature methods*, vol. 8, no. 1, pp. 26–29, 2011.
[13] H.-H. Wang, M. Krstić, and G. Bastin, "Optimizing bioreactors by extremum seeking," *International Journal of Adaptive Control and Signal Processing*, vol. 13, no. 8, pp. 651–669, 1999.
[14] C. Baroukh, F. Mairet, and O. Bernard, "The paradoxes hidden behind the droop model highlighted by a metabolic approach," *Front. Plant Sci*, 2022.
[15] R. J. Geider, H. L. Maclntyre, and T. M. Kana, "A dynamic regulatory model of phytoplanktonic acclimation to light, nutrients, and temperature," *Limnology and oceanography*, vol. 43, no. 4, pp. 679–694, 1998.